PERFORMANCE CHARACTERISTICS OF A VECTOR SENSOR ARRAY IN AN ENERGETIC TIDAL CHANNEL

Kaustubha Raghukumar, Grace Chang[a], Frank Spada[a], Craig Jones[a], Jesse Spence[b], Sean Griffin[c], Jesse Roberts[d]

[a]Integral Consulting Inc., 200 Washington Street, Suite 201, Santa Cruz, CA 95062, USA
[b]Noise Control Engineering, LLC**,** 799 Middlesex Turnpike, Billerica, MA 01821, USA
[c]Proteus Technologies, 1040 Old Spanish Trail, Suite 7, Slidell, LA 70458, USA
[d]Sandia National Laboratories, P.O. Box 5800, Albuquerque, NM 87185-0101, USA

Kaustubha Raghukumar, 200 Washington Street, Suite 201, Santa Cruz, CA 95062 USA
Phone number: +1 831 466 9630, kraghukumar@integral-corp.com

Abstract: *A compact three-dimensional vector sensor array (termed the NoiseSpotter) was recently developed with the goal of characterizing and localizing sources of sound in energetic environments such as those where marine renewable energy devices are likely to be located. The three vector sensors on the NoiseSpotter are mounted on a bottom platform with each sensor suspended inside an optional flow noise removal shield. The multiple pressure and particle velocity channels on the NoiseSpotter are simultaneously sampled and stored on-board to enable coherent array processing of vector sensor array data.*

A series of field trials were conducted where the NoiseSpotter was deployed on a bottom platform in an 8 m deep tidal channel in Sequim Bay, Washington. Pure tones were transmitted from a drifting vessel whose distance from the bottom platform varied between 50 m and 500 m. The effect of flow noise on vector sensor array performance is quantified along with the detectability of low intensity sound in an energetic environment. Flow noise removal efficiency for each channel of every vector sensor is demonstrated using multiple metrics derived from the active and reactive intensities computed using the pressure-velocity cross-spectral density matrix. A flow noise removal shield is shown to improve the detectability of low intensity sound such as those that are expected to be emitted by marine renewable energy devices.

Keywords: *vector sensor array, particle motion, marine renewable energy, flow noise*

1. INTRODUCTION

In support of monitoring technologies to evaluate the potential environmental effects of marine and hydrokinetic (MHK) energy devices, a compact three-dimensional array of acoustic vector sensors (termed the NoiseSpotter) was developed that characterizes, classifies, and provides accurate location information for anthropogenic and natural sounds. By virtue of measuring the acoustic pressure and three-dimensional particle velocity, a vector sensor array (VSA) provides a compact means of achieving sound source localization, and thereby help characterize sound specific to a source [1]. This localization ability is key to characterizing sounds from MHK devices, which have been found to emit low intensity sounds on the order of 106-109 dB re 1 µPa in the frequency band 125-250 Hz and undetectable above the ambient noise outside this band [2].

Operational deployments of the NoiseSpotter are likely to occur in ocean regions with energetic flows induced by wave- or tidally-induced currents. The strong flows can induce non-acoustic pressure fluctuations that lead to contamination of acoustic signals. Flow noise contamination can be particularly acute with vector sensors due to saturation of the built-in accelerometer signal by energetic flows.

To facilitate NoiseSpotter deployments in energetic environments, a flow noise removal shield was developed and tested in a tidal channel in Washington, USA. Using a series of controlled source playbacks, the efficiency of the flow noise removal system is demonstrated using quantitative metrics that utilize the off-diagonal elements of the pressure-velocity cross spectral density matrix.

2. BACKGROUND

Vector sensor measurements consist of four measured quantities that represent acoustic pressure and particle velocity, represented as $\mathbf{A}(\boldsymbol{x},t) = [p, v_x, v_y, v_z]$, where the particle velocity components are expressed in units of pressure via the scaling ρc, where ρ is the density of sea water (1000 kg/m^3), and c is the nominal speed of sound in sea water (1500 m/s). Velocity components are typically measured in a local frame of reference and transformed to an earth-based frame of reference using Eulerean angles measured by an in-built or collocated inertial motion unit.

The Fourier transform of the time series in $\mathbf{A}(\boldsymbol{x},t)$ is given by $\mathbf{A}(\boldsymbol{x},\omega)$. The cross-spectral density matrix $\mathbf{S}(\omega)$ is then given by the ensemble-averaged outer product of the vector $\mathbf{A}(\boldsymbol{x},\omega)$. Individual components of the cross-spectral density matrix can be expressed as $S_{ij}(\mathbf{x},\omega) = A_i(\mathbf{x},\omega)A_j^*(\mathbf{x},\omega)$. Assuming ergodicity, $\mathbf{S}(\mathbf{x},\omega)$ can be calculated by averaging successive snapshots of $\mathbf{A}(\boldsymbol{x},\omega)$ computed over an interval of time. $\mathbf{S}(\mathbf{x},\omega)$ can then be decomposed into its real and imaginary components as $\mathbf{S}(\mathbf{x},\omega) = \mathbf{C}(\mathbf{x},\omega)+i\ \mathbf{Q}(\mathbf{x},\omega)$, where $\mathbf{C}(\mathbf{x},\omega)$ and $\mathbf{Q}(\mathbf{x},\omega)$ represent the in-phase and quadrature components of the individual elements of the cross-spectral density matrix. For example, the off-diagonal elements $\mathbf{S}_{1j}(\mathbf{x},\omega)$ represent the pressure-velocity cross-spectra whose in-phase and quadrature elements have been related to physical quantities that represent acoustic power flow [3]. The in-phase components $\mathbf{C}_{1j}(\mathbf{x},\omega)$, termed the ***active intensity***, represents the net power being propagated by the acoustic field. The quadrature component, $\mathbf{Q}_{1j}(\mathbf{x},\omega)$, termed the ***reactive intensity***, relates pressure and particle velocity components that are orthogonal to each other, and represents spatially heterogeneous power flow [3].

A number of metrics to describe the non-acoustic contributions to acoustic propagation can be derived using the reactive intensity components of the cross-power spectral density matrix. For example, one can derive the metric [4],

$$R_j \equiv \frac{\rho_0 c_0 Q_{1j}(\omega)}{C_{11}(\omega)}, \tag{1}$$

where R_j is the scaled ratio of the reactive intensity to the acoustic pressure autospectrum. For propagating acoustic signals, the metric R_j when sampled over time can be expected to cluster around a mean value, where the magnitude of this mean value depends on the level of spatial heterogeneity in the signal. In the event of non-acoustic contamination by flow noise, the phase relationship between the pressure and particle velocity signals is random and the distribution of R_j is uniformly spread over a range of values. Therefore, an examination of the distribution of R_j can provide an indication of the degree of non-acoustic contamination.

An additional metric to evaluate the contribution of the non-acoustic component can be defined [4] that arises from the relationship between the particle velocity cross-spectra and active and reactive intensity vectors:

$$M_{21} = \frac{|Q_{34}(\omega)| - \left|\left(\frac{C_{1[2,3,4]}(\omega) \times Q_{1[2,3,4]}(\omega)}{S_{11}(\omega)}\right)_x\right|}{|Q_{34}(\omega)| + \left|\left(\frac{C_{1[2,3,4]}(\omega) \times Q_{1[2,3,4]}(\omega)}{S_{11}(\omega)}\right)_x\right|},$$

$$M_{22} = \frac{|Q_{42}(\omega)| - \left|\left(\frac{C_{1[2,3,4]}(\omega) \times Q_{1[2,3,4]}(\omega)}{S_{11}(\omega)}\right)_y\right|}{|Q_{42}(\omega)| + \left|\left(\frac{C_{1[2,3,4]}(\omega) \times Q_{1[2,3,4]}(\omega)}{S_{11}(\omega)}\right)_y\right|}, \tag{2}$$

$$M_{23} = \frac{|Q_{23}(\omega)| - \left|\left(\frac{C_{1[2,3,4]}(\omega) \times Q_{1[2,3,4]}(\omega)}{S_{11}(\omega)}\right)_z\right|}{|Q_{23}(\omega)| + \left|\left(\frac{C_{1[2,3,4]}(\omega) \times Q_{1[2,3,4]}(\omega)}{S_{11}(\omega)}\right)_z\right|}.$$

The notation $X_{1[2,3,4]}$ represents the off-diagonal elements of the matrix **X**, arranged as a vector, and '×' is the vector cross-product. Values of M_{2j} that deviate significantly from zero are considered to be a flag of non-acoustic contamination.

3. EXPERIMENT

The VSA was deployed at the mouth of Sequim Bay in Washington, USA on a bottom platform in a water depth of 8 m with respect to the mean sea level. This location is an energetic tidal channel, where the tidal excursion during the deployment was 2.5 m. Sensors on the VSA consisted of two Geospectrum M20-040 vector sensors and one Geospectrum M020-100 vector sensor that also measures sensor orientation. In this paper, sensor data from the M20-100 are analysed for flow noise contamination. The sensors are sensitive to acoustic frequencies in the 50 Hz- 5 kHz range, with a flat frequency response on the pressure channel, and a peak in the response at 1 kHz on the particle velocity channels. The flow noise shields were constructed of 1050 ballistic nylon wrapped around a baffled PVC tube in which a vector sensor was suspended. The flow shield was in place during an outgoing tide (Figure 1), and removed from the PVC baffle during the subsequent rising tide. Low-frequency

sinusoidal pulses and frequency sweeps were transmitted using a sound source on board a boat that drifted past the sensor platform at distance that ranged from 50 m to 500 m.

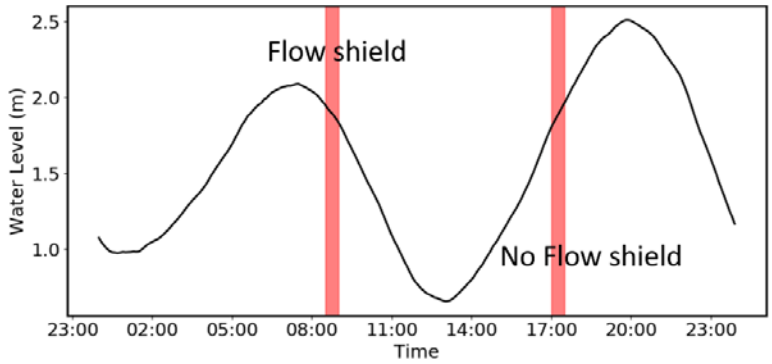

Figure 1: Tidal water level over the course of the field test on August 30, 2018.

4. RESULTS

Particle velocity and pressure frequency spectra were calculated with and without the flow noise removal shield (Figure 2).

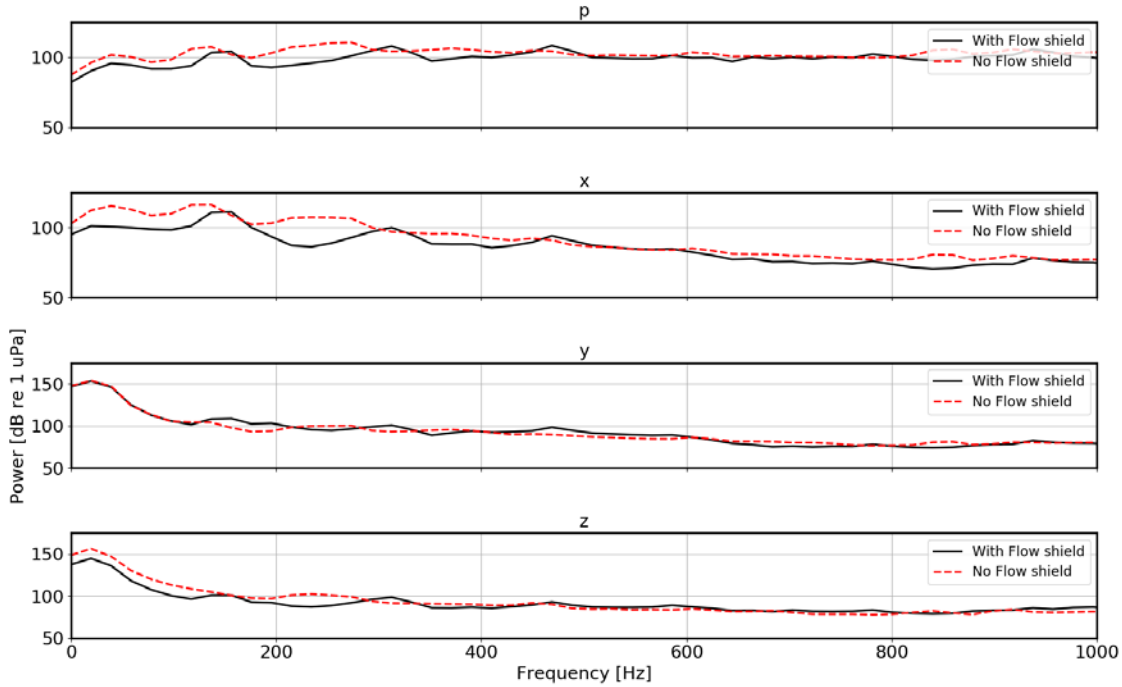

Figure 2: Frequency spectra for the pressure and particle velocity channels, with and without the flow shield.

Improvements in flow noise reduction are seen in the primary flow noise frequency band of 0-500 Hz on the pressure, x-, and z-particle velocity channels. Little to no change is observed for the y-particle velocity channel, attributed to the flow being orthogonal to the y-axis.

The probability distribution of R_j (Equation 1) is computed over a 30-minute period during each tidal cycle and is shown in Figure 3. The distribution markedly clusters around zero for the x-channel with the flow shield, consistent with the lowering of flow noise seen in the frequency spectra (Figure 2). No improvements are seen on the y-channel, while improvements in the z-channel are seen below 100 Hz where the R_j distribution without the flow shield is somewhat more randomly distributed than that without the flow shield. In general, low mean values of the R_j indicate a spatially homogeneous signal.

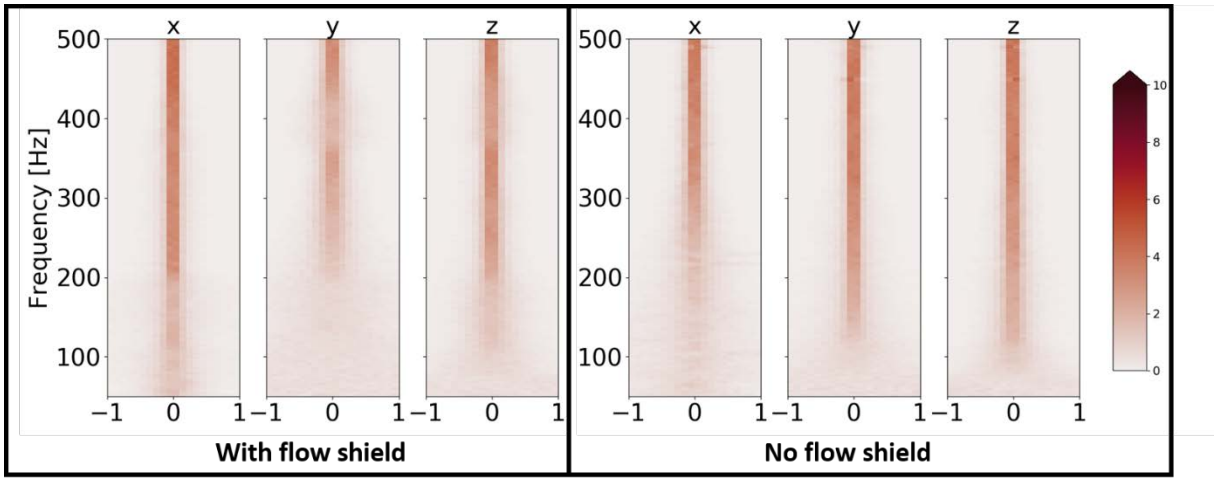

Figure 3: Probability distribution of R_j metric, with and without a flow shield.

Figure 4 shows the probability distribution of the M_{2j} metric, with and without the flow shield. A marked contrast is seen in the distributions with and without the flow shields. Distributions with the flow shield are seen to cluster around zero between 0-250 Hz, and no significant deviations towards higher values are observed. In contrast, the M_{2j} distributions without the flow shield are seen to cluster towards a value of 1 over much of the 0-500 Hz range shown, indicating the presence of non-acoustic signal contamination.

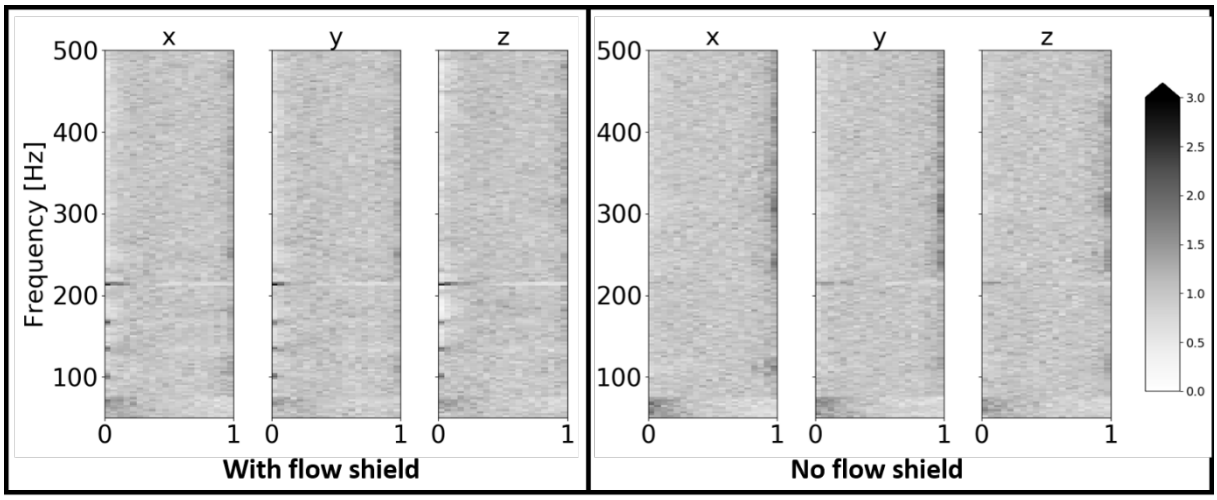

Figure 4: Probability distribution of M_{2j} metric, with and without a flow shield.

Figure 5 compares spectrograms of frequency sweeps as received on the pressure channel of a vector sensor, which illustrates the significant signal degradation in the absence of the flow noise removal shield. A visibly higher noise floor is seen in the absence of the flow shield, indicating significant degradation of signal detectability in the absence of the flow shield. Of particular interest is the low frequency portion of the spectrogram where the presence of a flow shield noticeably lowers the low frequency noise floor.

5. CONCLUSIONS

A field test of a vector sensor array was conducted in an energetic tidal channel where controlled source sweeps were transmitted over a full tidal cycle. Efficiency of a flow noise shield is demonstrated using analytical metrics [3,4] of vector sensor measurements of pressure and particle velocity. Improvements in the spectral levels and probability

distributions of the reactive ratio are observed. Spectrogram signal-to-noise and particle velocity cross-spectral metrics show significant improvements with the flow shield installed. Use of the flow shield on vector sensor arrays in energetic ocean environments is critical to improving acoustic measurements

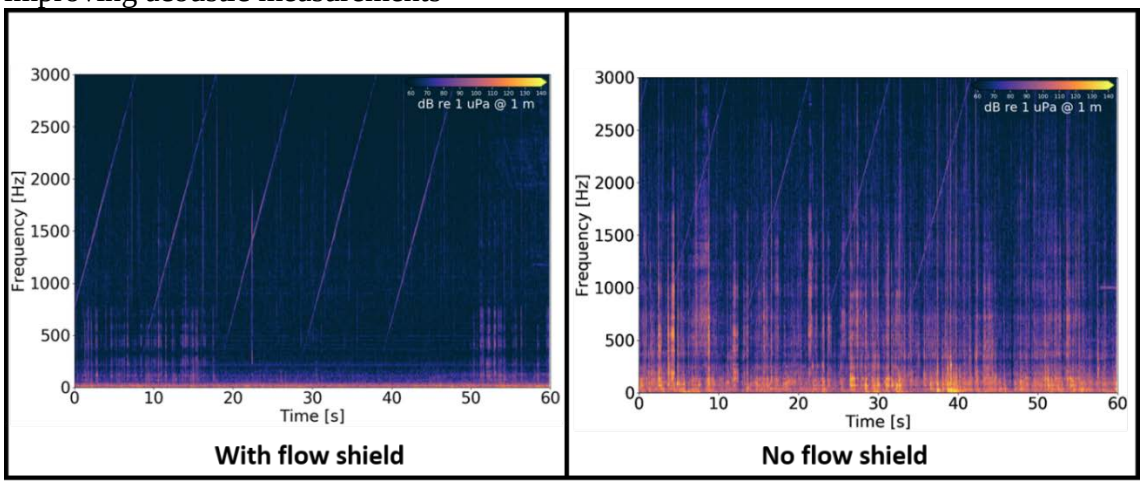

Figure 5: Received controlled source transmissions on the pressure channel of the vector sensor, with and without the flow shield.

6. ACKNOWLEDGEMENTS

The authors would like to thank the staff and crew at Pacific Northwest National Laboratories for a successful field effort. This material is based on work supported by the U.S. Department of Energy's Office of Energy Efficiency and Renewable Energy under the Water Power Program Award Number DE-EE0007822. This was prepared as an account of work sponsored by an agency of the United States Government. Neither the United States Government nor any agency thereof, nor any of their employees, makes any warranty, express or implied, or assumes any legal liability or responsibility for the accuracy, completeness, or usefulness of any information, apparatus, product, or process disclosed, or represents that its use would not infringe privately owned rights. Reference herein to any specific commercial product, process, or service by trade name, trademark, manufacturer, or otherwise does not necessarily constitute or imply its endorsement, recommendation, or favoring by the United States Government or any agency thereof. The views and opinions of authors expressed herein do not necessarily state or reflect those of the United States Government or any agency thereof.

REFERENCES

[1] Santos, P., Felisberto, P., and Hursky, P. Source localization with vector sensor array during the Makai Experiment, In *2nd International Conference and Exhibition on "Underwater Acoustic Measurements: Technologies and Results"*, Heraklion, Greece, 25–29 June 2007; pp. 985–990.

[2] Tougaard, J. 2015. Underwater noise from wave energy converters is unlikely to affect marine mammals. PloS One 10(7):e0132391

[3] D'Spain, G. 1990. Energetics of the deep ocean's infrasonic sound field. Ph.D. thesis, University of California, San Diego.

[4] Thode, A., Skinner, J., Scott, P., Roswell, J. 2010. Tracking sperm whales with a towed acoustic sensor. J. Acoust. Soc. Am. 128(5), 2681-2694.